RSC Advances

PAPER

View Article Online
View Journal | View Issue

Cite this: *RSC Adv.*, 2021, **11**, 24320

Tetramethylpyrazine: an electrolyte additive for high capacity and energy efficiency lithium–oxygen batteries†

Mengyuan Song,[a] Chunguang Chen,*[ab] Tao Huang[c] and Aishui Yu *[a]

Lithium–oxygen batteries have attracted great attention in recent years owing to their extremely high theoretical energy density, however, factors such as low actual capacity and poor rate performance hinder the practical application of lithium–oxygen batteries. In this work, a novel electrolyte additive, tetramethylpyrazine (TMP), is introduced into an electrolyte system to enhance the electrochemical performance of the lithium–oxygen batteries. TMP does not undergo its own redox reaction within the charge–discharge voltage range, which will not affect the electrochemical stability of the electrolyte. The results show that the addition of TMP can increase the reduction current of oxygen, which will promote the ORR process, and with an optimal TMP content (50 mM), the cell shows a high discharge capacity of 5712.3 mA h g^{-1} at 0.1 mA cm^{-2}. And its rate capability is almost doubled compared with the system without TMP additive at a large current density of 1 mA cm^{-2}. Further analysis by SEM and XRD reveals that the addition of TMP can reduce the formation of by-products and promote the solution growth of large-size Li_2O_2 particles to achieve a large discharge capacity. This approach could provide a new idea for improving the electrochemical performance of lithium–oxygen batteries.

Received 25th April 2021
Accepted 1st July 2021

DOI: 10.1039/d1ra03220h

rsc.li/rsc-advances

Introduction

Lithium–oxygen batteries (LOBs), based on their extremely high theoretical energy density, are an attractive electrical energy storage technology.[1–3] However, before this system can be used as a practical energy storage device, many challenges still need to be overcome, such as low actual capacity, poor rate performance, unsatisfactory energy efficiency, and the decomposition of electrolyte.[1–6] Efforts have been made to solve these problems: for example, noble metal catalysis,[7–9] the application of solid-state electrolytes[10,11] and electrode protection.[12] The most common method is the introduction of additives. On the one hand, they can be used as soluble redox mediators (RMs).[13,14] Since the Bruce group first reported TTF (tetrathiafulvalene) as RM in 2013,[15] a variety of RMs have been developed. For example, DBBQ (2,5-di-*tert*-butyl-1,4-benzoquinone),[16] TEMPO (2,2,6,6-tetramethylpiperidinyloxy),[17,18] DBDMB (2,5-di-*tert*-butyl-1,4-dimethoxybenzene)[19] and halides.[20,21] These RMs participate in the reaction of LOB with their own redox pairs to promote the progress of the reaction. On the other hand, the additives can optimize the properties of the electrolyte.[22–24] A large number of studies have shown that the discharge capacity and rate performance of LOB are greatly related to the physical properties of the electrolyte, including the ionic conductivity, viscosity, and oxygen solubility.[22,25–27] And increasing the solvation of Li^+ can increase the solubility of the lithium superoxide produced in the first step of the reaction in the solution.[28] That is, oxygen can be first adsorbed on the surface of the electrode during the discharge process and further obtains electrons and then reacts with Li^+ to form a soluble intermediate $LiO_{2(sol)}$. The $LiO_{2(sol)}$ intermediate can be further reduced on the surface or through a disproportionation reaction without electrons to form the final product Li_2O_2.[29,30]

Different from the intercalation mechanism of traditional lithium-ion batteries, the electrochemical reaction of LOB is based on the reaction between lithium metal and O_2, that is, the formation and decomposition reaction of the product Li_2O_2.[3] Two pathways for the growth of Li_2O_2 have been proposed: surface mechanism and solution mechanism.[30] The product obtained from surface mechanism is a thin film adhered to the surface of the electrode which will passivate the cathode due to the insulation of Li_2O_2, resulting in low discharge capacity and poor cycle performance.[31,32] In contrast, solution mechanism can provide large-sized Li_2O_2 with a higher discharge capacity. Therefore, promoting solution mechanism of Li_2O_2 is the key to increase the actual discharge capacity.

Here, we investigated the feasibility of a pyrazine organic compound, tetramethylpyrazine (TMP), as an electrolyte additive. TMP has basic properties similar to pyridine. Its two

[a]Department of Chemistry, Fudan University, Shanghai, 200438, China. E-mail: asyu@fudan.edu.cn
[b]Department of Chemistry, College of Science, University of Shanghai for Science and Technology, Shanghai 200093, China. E-mail: cgchen19@usst.edu.cn
[c]Laboratory of Advanced Materials, Fudan University, Shanghai, 200438, China

† Electronic supplementary information (ESI) available. See DOI: 10.1039/d1ra03220h

nitrogen atoms are located in the para position of the large conjugated π-type ring, thus the basicity becomes weaker due to mutual electron attraction. Its unique property can increase the solvation of Li^+ and the amount of dissolved oxygen in the system. In addition, the system containing TMP promotes the generation of Li_2O_2, and reduces the generation of by-products. In this work, TMP was used as a new additive in TEGDME electrolyte. The relevant physical and electrochemical properties of this new electrolyte system were systematically studied, and the reasons for its influence on the discharge capacity and rate performance of LOB were discussed.

Results and discussion

Physical and electrochemical properties of TMP added to the electrolyte

Fig. 1a shows the physical properties of different electrolytes. The increase of the TMP content does not have a major impact on the viscosity (Fig. S1†). But TMP increases the ionic conductivity of the system, which will have a vital impact on the discharge performance. At the same time, the addition of TMP significantly increases the amount of dissolved oxygen, and the higher oxygen solubility will improve the discharge capacity and rate performance to a certain extent.[22,27] Moreover, the chemical shift of ^{7}Li NMR increases as the amount of TMP increases (Fig. 1b), indicating there is a strong interaction between TMP and Li^+, or in other words, Li^+ can be solvated by TMP.[19,23,33]

The influence of the addition of TMP on the electrochemical performance was determined by cyclic voltammetry (CV) measurements in a three-electrode electrochemical cell. No additional peaks appears under the condition of argon or oxygen atmosphere (Fig. 1c and S2†), which means that TMP does not undergo its own oxidation–reduction reaction within the studied voltage range. That is, TMP will not affect the electrochemical stability of the electrolyte. As shown by the black trace in Fig. 1c, under oxygen condition, the cathodic current starts to flow at around 2.75 V with a broad reduction peak in the negative-going sweep, which can be attributed to the electrochemical reduction of O_2. And the introduction of TMP into the electrolyte increases the reduction current of oxygen, indicating that TMP has a certain positive effect on the oxygen reduction reaction (ORR), and the system containing 50 mM TMP has the most significant effect. Fig. S3† provides the electrochemical impedance spectra (EIS) of cells with different TMP content at an open circuit potential in an oxygen atmosphere. Since the overpotential is mainly related to the kinetic properties of the cell itself (the interface impedance between the electrode and the electrolyte), these results indicate that the addition of TMP reduces the R_{ct} and promotes the ORR dynamic activity. Moreover, the discharge platform (about 2.75 V) is not affected by the addition of TMP, revealing that the electrochemical reduction step of oxygen on the positive electrode surface is independent of the presence of TMP (Fig. 1d). And it has a certain positive effect on decreasing the charge plateau. These results are in good agreement with the conclusions of CV and EIS.

Rotating ring-disk electrode (RRDE) experiment was carried out to verify the influence of TMP on the growth mechanism of Li_2O_2 during the discharge process (Fig. 2). In the electrolyte without TMP, the disk and ring current at 2500 rpm are less than the currents at 1600 rpm, which reflects that the disk and ring current do not show a positive correlation at high speeds. The low-DN solvent TEGDME has a weak solvation effect on Li^+, leading to the surface growth of Li_2O_2, and the passivation of the disk electrode causes the current to deviate from the theoretical trend. However, when 50 mM TMP is introduced, the disk current keeps increasing with the increase of the rotation speed, revealing that the solution phase pathway is dominant.[19,34–36]

Electrochemical performance of the LOB

To further investigate the effects of TMP on discharge performance, cells containing different amounts of TMP were discharged at different current densities ranging from 0.1 to 1 mA cm^{-2}. As shown in Fig. 3a–d, the addition of TMP enhances the discharge capacity, and this trend increases as the current

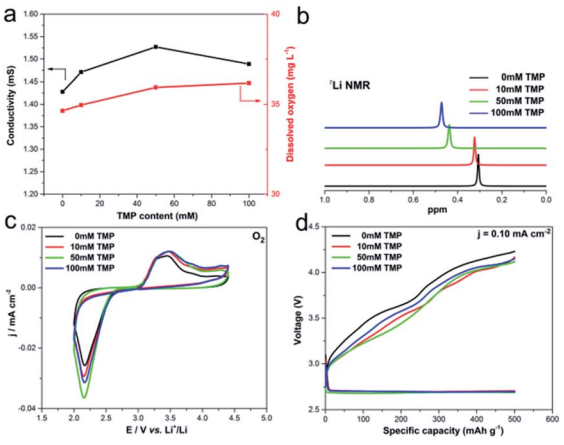

Fig. 1 (a) Ionic conductivity and dissolved oxygen, (b) ^{7}Li NMR spectra, (c) cyclic voltammograms under O_2 atmosphere at 50 mV s^{-1} and (d) first cycle at a constant current density of 0.1 mA cm^{-2} in 0.5 M LiTFSI/TEGDME with various amounts of TMP content.

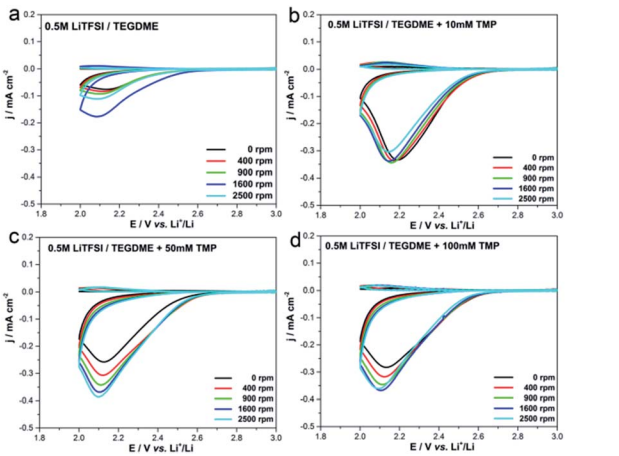

Fig. 2 RRDE test of electrolytes with various amounts of TMP at scan rate of 50 mV s^{-1} and ring potential of 3.5 V.

density increases. When the current density is 0.1 mA cm^{-2}, the discharge capacity of the electrolyte without TMP is 4907 mA h g^{-1}, while the discharge capacity of the electrolyte containing 10 mM, 50 mM, and 100 mM TMP are 5087.7, 5712.3, and 5492.4 mA h g^{-1}, respectively. And the discharge capacity of the electrolyte containing 10 mM, 50 mM, and 100 mM TMP are 545.9, 628.8, 594.3 mA h g^{-1}, which is almost twice as much as the electrolyte without TMP (276.7 mA h g^{-1}) at a current density of 1 mA cm^{-2}. Fig. 3e shows the percentage of the discharge capacity at different current densities to the discharge capacity at a current density of 0.1 mA cm^{-2}. According to Fig. 3e, the rate capability of the cell containing TMP additive is higher than that of the cell without TMP additive.[6,23] The amount of dissolved oxygen and ionic conductivity play a leading role at low and high current density respectively, and TMP has a positive effect on both.[25,26] Therefore, the influence of this additive on cell performance depends on the combination of TMP's promotion of these two influences. In addition, the discharge platform of the cell containing TMP increases and this phenomenon is more obvious at high current density, confirming that the addition of TMP reduces R_{ct} of the cell and increases the ORR dynamic activity, which is consistent well with EIS discussed above. This also provides evidence that the second reduction step from O_2^- to Li_2O_2 may be influenced by TMP during the discharge process at high current density. Furthermore, the influence of TMP on the long-term cycle stability of the cell was also tested (Fig. S4†). The addition of TMP slightly improves the cycling performance of the cell, which can also reflect that TMP is relatively stable during the cycle.

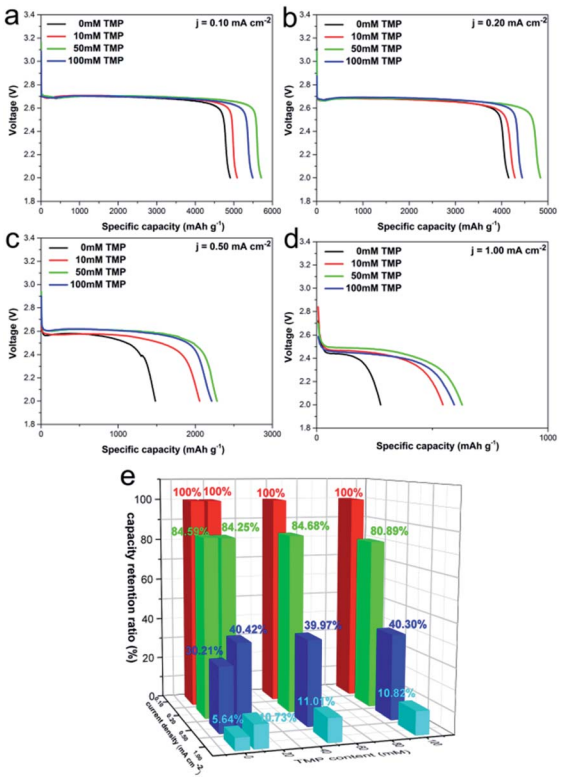

Fig. 3 (a–d) Discharge curves of LOB at different current densities and (e) capacity retention of the cells with various amounts of TMP content.

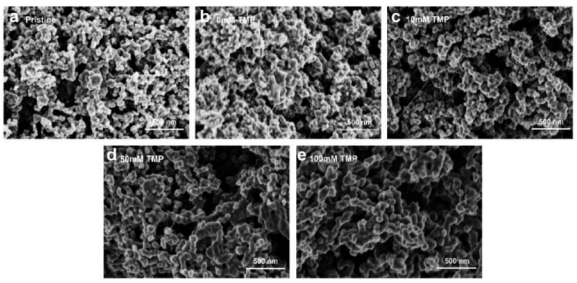

Fig. 4 SEM images of (a) pristine electrode and (b–e) the electrode after first discharge of the cells with various amounts of TMP content at a current density of 0.1 mA cm^{-2}.

Characterization of discharge products

To investigate the reason for the changes in the cell performance (such as capacity and rate performance), the discharged cathodes were examined by scanning electron microscopy (SEM). The results were shown in Fig. 4. Compared with the pristine cathode (Fig. 4a), in the absence of TMP, a mass of clumps accumulates on the surface of the electrode, which mainly derives from the decomposition product of the electrolyte, and the by-products covering the cathode almost block the pores of the electrode. In contrast, after adding 10 mM TMP, the amount of polymer on the surface decreases. With the increase of TMP addition, the discharge products uniformly cover the surface of the positive electrode, resulting in a film-like discharge product, and larger size products gradually form on the electrode surface. The change in the morphology of the discharge product is mainly due to the different discharge reaction mechanism caused by the difference of the electrolyte system. And the solution phase mechanism is more likely to generate large-size Li_2O_2 to obtain higher discharge capacity. To better understand the TMP effect in LOB, its influence on discharged products in a ether-based LiTFSI-TEGDME system was shown in Fig. 5. As mentioned above, TMP and Li^+ have a strong interaction, which will promote the solution growth mechanism of Li_2O_2, resulting in a higher discharge capacity.[28,32] After adding 100 mM TMP, it can be seen that the surface of the

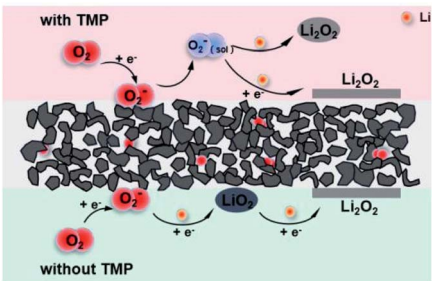

Fig. 5 Mechanism diagram of TMP in LOB.

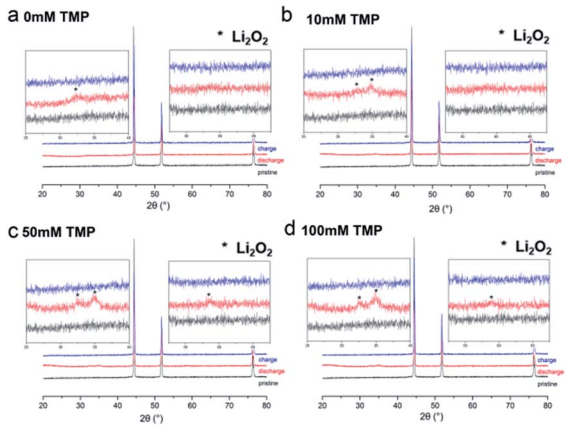

Fig. 6 XRD patterns of pristine, discharged and recharged cathodes.

positive electrode is almost completely covered by the film, and almost no spherical product is observed. Due to the passivation of the electrode by the insulating and insoluble products, the discharge performance of the cell would be affected.[31] That is, when the TMP content is 100 mM, the increase in the specific capacity is modest.

To demonstrate that the particles observed in SEM were indeed Li_2O_2, X-ray diffraction (XRD) was performed on the discharged cathodes. The results were presented in Fig. 6. Only the peaks related to Li_2O_2 are observed in the XRD pattern. It is worth mentioning that the film-like Li_2O_2 obtained from the surface mechanism is amorphous, while the product formed by the solution mechanism is crystalline. Furthermore, the sharpness and intensity of the peaks increase with the increase of the amount of TMP, indicating that TMP can promote the formation of large crystalline Li_2O_2 particles. The infrared spectrum in Fig. 7 confirms that the addition of TMP reduces the formation of by-products. Although low-DN TEGDME is relatively stable, it still decomposes during the cycling.[37–39] Therefore, peaks of electrolyte decomposition products (such as lithium carbonate and lithium formate) appear in the infrared spectrum. In the system without TMP, the peaks of these by-products (mainly lithium carbonate) are strong and clear, which proves that the degree of decomposition of the electrolyte is greater, similar to the results of SEM. After adding TMP, the peaks of these by-products are significantly reduced, and the peak intensity is weakened, indicating that the film formed by TMP on the surface of the positive electrode reduces the decomposition of the electrolyte to a certain extent.

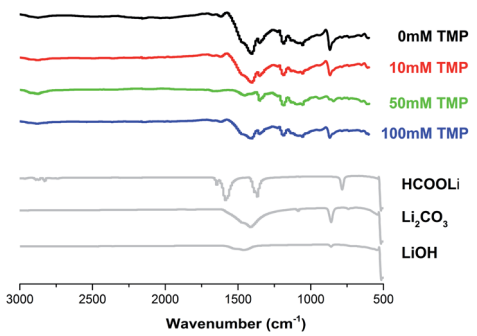

Fig. 7 IR spectra of pristine, discharged and recharged cathodes.

Conclusions

In summary, a chemical and electrochemical stable TMP additive in electrolyte has great effect on enhancing the discharge capacity and rate performance of LOB. The increasing of ionic conductivity and dissolved oxygen content in electrolyte by TMP additive are beneficial to the electrochemical performance, could lead to charge transfer impedance reducing and ORR kinetics increasing. When an optimal TMP content (50 mM) is added in the electrolyte, the discharge capacity reaches 5712.3 mA h g^{-1} at 0.1 mA cm^{-2}, and 628.8 mA h g^{-1} at relative high current density of 1 mA cm^{-2}. The rate capability of the cell is greatly improved, with the optimal TMP content, the capacity at 1 mA cm^{-2} is more than twice that of the cell without the TMP additive. These improvements are attributed to the strong interaction between TMP and Li^+, which improves the solubility of reaction intermediates and promotes the solution mechanism of Li_2O_2. With TMP in electrolyte, the electrochemical reaction route could be different, since it can change the morphology of the discharge products from film to spherical and reduce the formation of by-products. TMP could be a promising additive in LOB and further works on tuning TMP-like structure for more effective additives is still going on.

Experimental

Electrolyte preparation

Tetraethylene glycol dimethyl ether (TEGDME, Aladdin, 99%) solvent was dried over activated 4 Å molecular sieves for 3 days to remove residual water. The salt of lithium bis(trifluoromethane)sulfonimide (LiTFSI, 99%) was purchased from Aladdin. The lithium salt concentration was 0.5 M. The electrolyte composed of 0.5 M LiTFSI in TEGDME was regarded as the basic system, and different amounts of TMP (Aladdin, 98%) were added to the above solution to obtain *x*TMP-based electrolyte (x = 0, 10, 50, 100 mM). Since the preparation of the electrolyte had a particularly high requirement for water and oxygen, thus all preparation operations were completed in a glove box filled with argon ($H_2O \leq 0.1$ ppm, $O_2 \leq 0.1$ ppm).

Preparation of electrode and cell assembly

Ketjen black (KB) and 20 wt% polytetrafluoroethylene (PTFE) were mixed with a weight ratio of 8 : 2, and were dispersed in the ethanol solution. The obtained slurry was uniformly coated on the nickel foam with a diameter of 12 mm. The electrode was dried for 12 h in a vacuum oven at 80 °C to remove residual solvent. The area mass of the active material KB loading on the electrode contacted with oxygen was approximately 0.83 mg cm^{-2}.

The investigated cells in this article were assembled using Swagelok-type cells containing a lithium foil, a separator (Celgard 3500), an as-prepared electrode and 100 μL *x*TMP-based electrolyte. In order to eliminate the influence of other

components in the air (especially water and carbon dioxide) on the cell test process, all lithium–oxygen battery tests were carried out in a glove box filled with high purity oxygen ($H_2O \leq 0.1$ ppm).

Electrochemical tests and material characterization

The oxygen solubility and ionic conductivity of the electrolyte were measured by Oakton PCD650 multi-parameter water quality analyzer, and the viscosity was measured by a digital viscometer (NDJ-5S).

The charge and discharge tests were carried out at different current densities and in a voltage range of 2.0–4.4 V. In the cycle test, the charge and discharge capacity was limited to 500 mA h g^{-1}.

The surface structure and surface composition of the electrode after cycling were investigated by field emission scanning electron microscope (FESEM, JEOL JSM-6390) and X-ray diffraction (XRD, D8-Advanced X-ray diffractometer, Cu Kα, λ = 1.5406 Å).

Cyclic voltammetry (CV). CV experiments were performed in an airtight three-electrode electrolytic cell using lithium foil as the reference electrode, platinum as the counter electrode and a glassy carbon electrode with a diameter of 6 mm as the working electrode. Before each experiment, the glassy carbon electrode was carefully polished with 0.05 μm alumina powder. The electrolytic cell was assembled in a glove box filled with argon. After continuously injecting argon or oxygen into the system for 20 minutes, the CV experiments were latter performed using an electrochemical workstation (CHI 660D). The test voltage range was 2.0 V to 4.4 V and the scan rate was 50 mV s^{-1}. The CV test voltage interval was as the same as that of a normal cell.

Conflicts of interest

There are no conflicts to declare.

Acknowledgements

The authors acknowledge the financial support from the Natural Science Foundation of Shanghai (19ZR1403600), and Shanghai Science and Technology Committee (19DZ2270100), China.

Notes and references

1 J. Christensen, P. Albertus, R. S. Sanchez-Carrera, T. Lohmann, B. Kozinsky, R. Liedtke, J. Ahmed and A. Kojic, *J. Electrochem. Soc.*, 2011, **159**, R1–R30.
2 J.-S. Lee, S. Tai Kim, R. Cao, N.-S. Choi, M. Liu, K. T. Lee and J. Cho, *Adv. Energy Mater.*, 2011, **1**, 34–50.
3 C. Shu, J. Wang, J. Long, H. K. Liu and S. X. Dou, *Adv. Mater.*, 2019, **31**, e1804587.
4 B. D. Adams, R. Black, Z. Williams, R. Fernandes, M. Cuisinier, E. J. Berg, P. Novak, G. K. Murphy and L. F. Nazar, *Adv. Energy Mater.*, 2015, **5**, 1400867.
5 M. Christy, A. Arul, A. Zahoor, K. U. Moon, M. Y. Oh, A. M. Stephan and K. S. Nahm, *J. Power Sources*, 2017, **342**, 825–835.
6 A. Dutta, K. Ito and Y. Kubo, *J. Mater. Chem. A*, 2019, **7**, 23199–23207.
7 Y. Dou, R. Lian, Y. Zhang, Y. Zhao, G. Chen, Y. Wei and Z. Peng, *J. Mater. Chem. A*, 2018, **6**, 8595–8603.
8 M. Luo, Z. Zhao, Y. Zhang, Y. Sun, Y. Xing, F. Lv, Y. Yang, X. Zhang, S. Hwang, Y. Qin, J. Y. Ma, F. Lin, D. Su, G. Lu and S. Guo, *Nature*, 2019, **574**, 81–85.
9 Y.-C. Lu, Z. Xu, H. A. Gasteige, S. Chen, K. Hamad-Schifferli and Y. Shao-Horn, *J. Am. Chem. Soc.*, 2010, **132**, 12170–12171.
10 K. Liu, H. Sun, S. Dong, C. Lu, Y. Li, J. Cheng, J. Zhang, X. Wang, X. Chen and G. Cui, *Adv. Mater. Interfaces*, 2017, **4**, 1700693.
11 Y. Han, X. Zhang, B. Lu, Y. Li, C. Shao, Q. Guo and Z. Zhang, *Nano Futures*, 2020, **4**, 032005.
12 L. Ma, Z. Bi, Y. Xue, W. Zhang, Q. Huang, L. Zhang and Y. Huang, *J. Mater. Chem. A*, 2020, **8**, 5812–5842.
13 W. Zhao, X. Mu, P. He and H. Zhou, *Batteries Supercaps*, 2019, **2**, 803–819.
14 J. B. Park, S. H. Lee, H. G. Jung, D. Aurbach and Y. K. Sun, *Adv. Mater.*, 2018, **30**, 1704162.
15 Y. Chen, S. A. Freunberger, Z. Peng, O. Fontaine and P. G. Bruce, *Nat. Chem.*, 2013, **5**, 489–494.
16 X. Gao, Y. Chen, L. Johnson and P. G. Bruce, *Nat. Mater.*, 2016, **15**, 882–888.
17 X. Gao, Y. Chen, L. R. Johnson, Z. P. Jovanov and P. G. Bruce, *Nat. Energy*, 2017, **2**, 17118.
18 B. J. Bergner, A. Schurmann, K. Peppler, A. Garsuch and J. Janek, *J. Am. Chem. Soc.*, 2014, **136**, 15054–15064.
19 Q. Xiong, G. Huang and X. B. Zhang, *Angew. Chem., Int. Ed.*, 2020, **59**, 19311–19319.
20 H. D. Lim, H. Song, J. Kim, H. Gwon, Y. Bae, K. Y. Park, J. Hong, H. Kim, T. Kim, Y. H. Kim, X. Lepro, R. Ovalle-Robles, R. H. Baughman and K. Kang, *Angew. Chem., Int. Ed.*, 2014, **53**, 3926–3931.
21 W.-J. Kwak, D. Hirshberg, D. Sharon, H.-J. Shin, M. Afri, J.-B. Park, A. Garsuch, F. F. Chesneau, A. A. Frimer, D. Aurbach and Y.-K. Sun, *J. Mater. Chem. A*, 2015, **3**, 8855–8864.
22 H. Wan, Y. Mao, Z. Liu, Q. Bai, Z. Peng, J. Bao, G. Wu, Y. Liu, D. Wang and J. Xie, *ChemSusChem*, 2017, **10**, 1385–1389.
23 C. Chen, X. Chen, X. Zhang, L. Li, C. Zhang, T. Huang and A. Yu, *J. Mater. Chem. A*, 2018, **6**, 7221–7226.
24 Y. Wang, F. Bai, A. Wang, Z. Cui, D. Wang, S. Shi and T. Zhang, *Chem. Commun.*, 2021, **57**, 3030–3033.
25 J. Read, *J. Electrochem. Soc.*, 2002, **149**, A1190–A1195.
26 W. Xu, J. Xiao, J. Zhang, D. Wang and J.-G. Zhang, *J. Electrochem. Soc.*, 2009, **156**, A773–A779.
27 O. Wijaya, P. Hartmann, R. Younesi, I. I. E. Markovits, A. Rinaldi, J. Janek and R. Yazami, *J. Mater. Chem. A*, 2015, **3**, 19061–19067.
28 L. Johnson, C. Li, Z. Liu, Y. Chen, S. A. Freunberger, P. C. Ashok, B. B. Praveen, K. Dholakia, J. M. Tarascon and P. G. Bruce, *Nat. Chem.*, 2014, **6**, 1091–1099.

29 S. S. Zhang and J. Read, *J. Power Sources*, 2011, **196**, 2867–2870.
30 Z. Lyu, Y. Zhou, W. Dai, X. Cui, M. Lai, L. Wang, F. Huo, W. Huang, Z. Hu and W. Chen, *Chem. Soc. Rev.*, 2017, **46**, 6046–6072.
31 V. Viswanathan, K. S. Thygesen, J. S. Hummelshoj, J. K. Norskov, G. Girishkumar, B. D. McCloskey and A. C. Luntz, *J. Chem. Phys.*, 2011, **135**, 214704.
32 Z. Luo, Y. Li, Z. Liu, L. Pan, W. Guan, P. Liu and D. Wang, *ChemSusChem*, 2019, **12**, 4962–4967.
33 C. M. Burke, V. Pande, A. Khetan, V. Viswanathan and B. D. McCloskey, *PNAS*, 2015, **112**, 9293–9298.
34 Y. Wang, N.-C. Lai, Y.-R. Lu, Y. Zhou, C.-L. Dong and Y.-C. Lu, *Joule*, 2018, **2**, 2364–2380.
35 M. J. Trahan, I. Gunasekara, S. Mukerjee, E. J. Plichta, M. A. Hendrickson and K. Abraham, *J. Electrochem. Soc.*, 2014, **161**, A1706.
36 Y. Wang, N.-C. Lai, Y.-R. Lu, Y. Zhou, C.-L. Dong and Y.-C. Lu, *Joule*, 2018, **2**, 2364–2380.
37 R. Younesi, M. Hahlin, F. Björefors, P. Johansson and K. Edström, *Chem. Mater.*, 2012, **25**, 77–84.
38 J. P. Vivek, N. Berry, G. Papageorgiou, R. J. Nichols and L. J. Hardwick, *J. Am. Chem. Soc.*, 2016, **138**, 3745–3751.
39 S. A. Freunberger, Y. Chen, Z. Peng, J. M. Griffin, L. J. Hardwick, F. Barde, P. Novak and P. G. Bruce, *J. Am. Chem. Soc.*, 2011, **133**, 8040–8047.